Combustion and Flame 161 (2014) 2729–2737

Contents lists available at ScienceDirect

Combustion and Flame

journal homepage: www.elsevier.com/locate/combustflame

# Physicochemical effects of varying fuel composition on knock characteristics of natural gas mixtures

Sander Gersen [a,*], Martijn van Essen [a], Gerco van Dijk [a], Howard Levinsky [a,b]

[a] DNV-GL Oil & Gas, P.O. Box 2029, 9704 CA Groningen, The Netherlands
[b] Energy and Sustainability Research Institute, University of Groningen, Nijenborgh 4, 9747 AG Groningen, The Netherlands

ARTICLE INFO

*Article history:*
Received 15 November 2013
Received in revised form 21 February 2014
Accepted 31 March 2014
Available online 3 May 2014

*Keywords:*
Engine knock
Autoignition delay times
Natural gas
Hydrogen

ABSTRACT

The physicochemical origins of how changes in fuel composition affect autoignition of the end gas, leading to engine knock, are analyzed for a natural gas engine. Experiments in a lean-burn, high-speed medium-BMEP gas engine are performed using a reference natural gas with systematically varied fractions of admixed ethane, propane and hydrogen. Thermodynamic analysis of the measured non-knocking pressure histories shows that, in addition to the expected changes arising from changes in the heat capacity of the mixture, changes in the combustion duration relative to the compression cycle (the combustion "phasing") caused by variations in burning velocity dominate the effects of fuel composition on the temperature (and pressure) of the end gas. Thus, despite the increase in the heat capacity of the fuel–air mixture with addition of ethane and propane, the change in combustion phasing is actually seen to increase the maximum end-gas temperature slightly for these fuel components. By the same token, the substantial change in combustion duration upon hydrogen addition strongly increases the end-gas temperature, beyond that caused by the decrease in mixture heat capacity. The impact of these variations in in-cylinder conditions on the knock tendency of the fuel have been assessed using autoignition delay times computed using SENKIN and a detailed chemical mechanism for the end gas under the conditions extant in the engine. The results show that the ignition-promoting effect of hydrogen is mainly the result of the increase in end-gas temperature and pressure, while addition of ethane and propane promotes ignition primarily by changing the chemical autoignition behavior of the fuel itself. Comparison of the computed end-gas autoignition delay time, based on the complete measured pressure history of each gas, with the measured Knock-Limited Spark Timing shows that the computed delay time accurately reflects the measured knock tendency of the fuels.



## 1. Introduction

As a result of the globalization of the energy market and the drive towards sustainability, the chemical composition of gaseous fuels is becoming more diverse. For example, "rich" natural gases, which contain substantially higher fractions of non-methane hydrocarbons than the traditionally distributed pipeline gas, are being introduced into the gas infrastructure. Sustainable gases obtained from fermentation or gasification of biomass, which can contain substantial fractions of carbon dioxide, hydrogen and carbon monoxide are being considered for introduction into the gas supply. The different compositions of such "new" gases can impact the combustion behavior of end-use equipment. With an eye towards successfully incorporating this diversity of supply, it is necessary to assess the effects of the wider range of fuel compositions on end-use equipment quantitatively.

Gas-fueled reciprocating internal combustion engines are known to be sensitive to variations in fuel composition because of the possible occurrence of engine knock, caused by autoignition of unburned fuel–air mixture, the so-called end gas, ahead of the propagating flame in the cylinder. Mild engine knock increases fuel consumption and pollutant emissions, while severe knock can physically damage the engine [1], and as such should be avoided. The knock sensitivity of gas engines is a limiting design factor for power output, efficiency and the acceptable variation in fuel gas composition. Empirical methods analogous to the octane number for gasoline [2,3], such as a methane number [4], which often make use of a standard test engine, have been developed to classify natural gases with respect to their knock sensitivity. Since the autoignition behavior of fuels and the relative differences in autoignition

* Corresponding author. Fax: +31 50 5219858.
*E-mail address:* Sander.Gersen@dnvkema.com (S. Gersen).

http://dx.doi.org/10.1016/j.combustflame.2014.03.019
0010-2180/

between fuels depend strongly on the specific regime of temperature and pressure (e.g., [5–18]), the generality of the method for engine conditions other than those existing in the test engine is uncertain. Furthermore, empirical methods provide only limited insight in the physical/chemical origins of knock in engines, and are therefore of limited utility for the optimum design for knock-free engine operation when using a wide range of fuels. Elucidation of the microscopic details of the effects of fuel composition on cylinder processes can provide insight essential for engine design, and can also be used to derive a fundamentally sound method for determining the knock tendency of fuels.

Autoignition of the end gas is governed by chemical kinetics, and occurs when the rate of reaction and the rate of heat release in the end gas grow exponentially. The tendency of a fuel mixture to autoignite depends strongly upon the reactivity of the fuel itself, the equivalence ratio and the pressure and temperature conditions of the mixture. For example, studies performed in shock tubes and rapid compression machines, RCMs, (see, for example, [5,7–9,12–18]) showed that the autoignition delay time of methane-based fuels decreases significantly as a result of increasing the temperature and pressure, and the addition of higher hydrocarbons or hydrogen. A fundamental analysis of engine knock therefore requires detailed knowledge about the actual state of the end gas, as well as any changes in this state caused by varying composition. Since the state of the end gas is affected by the thermophysical properties of the mixture and rate of combustion [1,20], the trends observed in shock tubes and RCMs by themselves are insufficient to characterize changes in knock behavior with varying fuel composition. Furthermore, affected by mechanical compression and thermal compression caused by progressive consumption of the fuel–air mixture, the state of the end gas varies with time during the combustion cycle. To quantify the progress of autoignition under these conditions for different gas compositions, this temporal variation in the temperature and pressure of the end gas must be determined. Although the knock characteristics [19,20], combustion duration [21,22] and flame speed [23,24], of $CH_4$, $C_2H_6$, $C_3H_6$, $H_2$ and their mixtures have been studied individually, the available information is insufficient to assess the contributions of the individual changes in the knock behavior of the fuel.

In this paper we analyze the changes in autoignition delay time of the end gas caused by the changes in the reactivity of the fuel itself and those arising from changes in in-cylinder pressure and temperature experienced by the end gas upon changing gas composition. The changes in in-cylinder conditions are studied both theoretically and using data obtained from a practical engine fueled with a variety of (simulated) natural gases. The fractions of ethane, propane and hydrogen in the gases are varied systematically to illustrate the underlying principles. In addition, the gases studied have been ranked for knock resistance based on the experimental determination of knock and on an analysis using computed end-gas autoignition delay times. The ultimate goals of this work are to provide insight into the physical and chemical processes governing the effects of fuel composition on engine knock and to rank gases for knock resistance based on a physically correct representation of these effects.

## 2. Experimental procedure

A lean-burn, high-speed, turbo-charged, intercooled 6-cylinder gas engine (MAN) for combined-heat-and-power applications (CHP) was used in this study. Table 1 lists the key specifications of this engine. We remark here that this CHP system maintains constant equivalence ratio, engine speed and power output. The engine management system and further instrumentation allowed for precise adjustment, monitoring and acquisition of power output, fuel consumption, exhaust gas emissions, ignition timing, air–fuel-ratio and other relevant engine parameters.

The in-cylinder pressures in all cylinders were measured with Kistler type 6052 piezoelectric pressure sensors and a Kistler type 5011 charge amplifiers connected to a Smetec Combi-Pro indication system. A crankshaft-mounted pulse generator provided 0.1 °CA resolution for the cylinder pressure data acquisition. The Combi-Pro system was also used for knock detection through monitoring of the maximum amplitude of pressure oscillations in the high-pass-filtered cylinder pressure data in a window of consecutive cycles. Threshold settings used were 2 bar for the amplitude and 30 cycles for the window. For knock-limited spark timing (KLST) experiments ([20], see below), the knock limit was arbitrarily chosen to be one knock event or cluster of knock events within a 15 min steady-state test run. The Combi-Pro system also provided analyses of the combustion process, such as the phasing of the heat release, based on the pressure trace.

During the experiments, fuel for the test engine was delivered by a gas mixing unit. This unit allows on-stream variation of the fuel gas composition by independent adjustment of the flow rates of up to six source gas streams, with a maximum capacity of 4 MW. The fuel compositions used in the experiments consist of Dutch natural gas (DNG) mixed with increasing fractions of ethane and/or propane (Table 2), or hydrogen (Table 3). All mixture compositions were verified by gas chromatography.

Once the composition of the fuel/air mixtures at equivalence ratio $\varphi = 0.67$ and the other relevant cylinder parameters are set (Tables 2 and 3), the pressure traces of the gases under non-knocking condition are measured at a constant spark timing of 14° before top dead center (BTDC). Subsequently, the spark timing was gradually varied up to the point of the onset of borderline knock to determine the KLST.

## 3. Simulation procedure

Since knock in spark-ignited engines is an autoignition phenomenon, we simulate engine knock by modeling autoignition of the compressed end gas during the cycle using the SENKIN code [25], in the CHEMKIN II library [26]. To predict the occurrence of engine knock accurately, it is necessary to account for the effects of the piston motion and flame propagation on the pressure and temperature history of the end gas in the simulations. Since we focus here on gaining insight into autoignition during the engine cycle, we avoid complex calculations of flame propagation for the present, and derive the pressure and temperature history of the unburned end gas from the experimental engine measurements. As successfully applied previously [27,28], we assume that knock occurs in an adiabatic core of the unburned end gas. As shall be seen below, the engine results themselves point to challenges for the simulation of burn cycle that are necessary to predict engine knock, a priori. For each simulation we derive the specific volume of the end gas from a measured non-knocking pressure history, using

$$\int_{T_i(t_0)}^{T(t)} \frac{\gamma}{\gamma-1} d\ln T = \ln \frac{P(t)}{P_i(t_o)}, \tag{1}$$

and

$$\ln(CR(t)) = \ln\left(\frac{V_i(t_0)}{V(t)}\right) = \int_{T_i(t_0)}^{T(t)} \frac{1}{\gamma-1} d\ln T, \tag{2}$$

where $T_i$ and $P_i$ are the measured intake temperature and pressure, respectively, while $V_i$ is the specific volume of the unburned gas at the start of the compression stroke, derived from $T_i$ and $P_i$; $P(t)$ is the measured pressure of the unburned gas mixture, $T(t)$ is the temperature of the unburned gas mixture, and $V(t)$ is the time-varying

**Table 1**
Key specifications of DNV GL test engine.

| | |
|---|---|
| Engine make and type | MAN E2876LE302 |
| Engine configuration | – 6 Cylinder in-line<br>– Turbocharged<br>– Intercooled |
| Combustion system and combustion stoichiometry | – Mono-gas<br>– Open chamber<br>– Lean-burn |
| Rated power and speed (corresponding BMEP) | 208 kW at 1500 rpm (13.0 bar) |
| Bore × stroke | 128 × 166 mm |
| Compression ratio | 11.0:1 |

specific volume of the unburned mixture forming the (time-dependent) compression ratio (CR($t$)). The ratio of the temperature-dependent specific heat capacities of the unburned mixture ($C_p/C_v$) is $\gamma(T)$.

While the existence of an isentropically compressed adiabatic core of the unburned mixture in our engine is uncertain [1], we anticipate that use of the treatment of the unburned mixture by using the measured pressure trace in a similar fashion as done in previous studies [27,28], will yield faithful trends in knock propensity since any changes in non-adiabatic behavior with changing gas composition will be modest in comparison to the changes in combustion observed in this study.

The specific volume, the composition of the fuel/air mixture and the measured intake pressure and temperature are used as input in the simulations. One result is illustrated in Fig. 1, where we present the measured (non-knocking) pressure trace (averaged over 280 cycles), the simulated pressure trace computed from the specific volume and the simulated pressure trace at increased intake temperature. It will be clear that using input conditions from non-knocking conditions in accurate simulations *should not* yield autoignition, which is also seen in Fig. 1. To cause engine knock in the simulations, we artificially increase the intake manifold temperature of the mixture until knock occurs in the simulations [28]. We define knock in the simulations when autoignition of the unburned end gas occurs before the flame completely consumes the end gas. More specifically, in the simulations we increased the manifold intake temperature so that in the simulation of the reference fuel (Gas A in Table 2) autoignition occurs (arbitrarily) at the timing corresponding to 90% apparent heat release, which is derived from the pressure traces. The rapid increase in the simulated pressure trace in Fig. 1 shows "knock" at 90% heat release for Gas A, which required an increase in the simulated intake manifold temperature by 47 K. Simulations for fuels with a lower knock

**Table 2**
Engine conditions and composition of rich natural gases studied.

| | A (DNG) | B | C | D | E | F | G |
|---|---|---|---|---|---|---|---|
| $CH_4$ | 81.827 | 80.744 | 79.828 | 75.211 | 67.209 | 74.462 | 65.350 |
| $C_2H_6$ | 2.664 | 4.413 | 2.699 | 11.048 | 20.425 | 2.502 | 12.281 |
| $C_3H_8$ | 0.369 | 0.395 | 3.106 | 0.369 | 0.325 | 9.128 | 10.187 |
| n-$C_4H_{10}$ | 0.058 | 0.062 | 0.080 | 0.059 | 0.067 | 0.085 | 0.161 |
| i-$C_4H_{10}$ | 0.0 | 0.0 | 0.074 | 0.0 | 0.053 | 0.142 | 0.0 |
| n-$C_5H_{12}$ | 0.098 | 0.092 | 0.098 | 0.095 | 0.084 | 0.085 | 0.074 |
| $H_2$ | 0 | 0 | 0 | 0 | 0 | 0 | 0 |
| He | 0.048 | 0.047 | 0.047 | 0.044 | 0.039 | 0.045 | 0.037 |
| $N_2$ | 14.005 | 13.242 | 13.187 | 12.325 | 11.05 | 12.700 | 11.160 |
| $CO_2$ | 0.931 | 0.909 | 0.880 | 0.851 | 0.749 | 0.852 | 0.752 |
| $T_{intake}$ manifold, K | 366.0 | 366.4 | 366.4 | 366.9 | 366.3 | 366.0 | 366.5 |
| $P_{intake}$ manifold, bar | 2.16 | 2.11 | 2.15 | 2.11 | 2.09 | 2.11 | 2.07 |
| $\lambda$ | 1.558 | 1.552 | 1.552 | 1.550 | 1.554 | 1.549 | 1.559 |
| Shaft power, kW | 208.3 | 208.2 | 207.5 | 207.7 | 208.5 | 208.3 | 208.2 |
| LHV, MJ/m$^3$ | 31.633 | 32.529 | 33.566 | 34.627 | 37.784 | 37.105 | 40.984 |
| Wobbe, MJ/m$^3$ | 43.784 | 44.742 | 45.523 | 46.625 | 49.326 | 48.178 | 51.353 |
| KLST, °BTDC | 24.0 | 22.5 | 20.0 | 19.5 | 17.5 | 16.0 | 14.0 |
| MN, AVL | 91.8 | 87.3 | 80.4 | 78.6 | 69.7 | 67.2 | 61.5 |

**Table 3**
Composition of hydrogen/natural gas mixtures.

| | H (DNG) | I | J | K | L | M |
|---|---|---|---|---|---|---|
| $CH_4$ | 81.92 | 79.36 | 76.87 | 73.08 | 68.94 | 65.46 |
| $C_2H_6$ | 2.93 | 2.84 | 2.76 | 2.64 | 2.48 | 2.35 |
| $C_3H_8$ | 0.44 | 0.43 | 0.42 | 0.40 | 0.38 | 0.36 |
| n-$C_4H_{10}$ | 0.08 | 0.08 | 0.08 | 0.07 | 0.07 | 0.07 |
| i-$C_4H_{10}$ | 0.07 | 0.07 | 0.06 | 0.06 | 0.06 | 0.06 |
| n-$C_5H_{12}$ | 0.11 | 0.11 | 0.11 | 0.12 | 0.10 | 0.10 |
| $H_2$ | 0 | 3.14 | 6.18 | 10.86 | 15.94 | 20.19 |
| He | 0.02 | 0.04 | 0.04 | 0.04 | 0.01 | 0.00 |
| $N_2$ | 13.42 | 12.99 | 12.56 | 11.89 | 11.21 | 10.64 |
| $CO_2$ | 0.96 | 0.94 | 0.91 | 0.86 | 0.82 | 0.78 |
| $T_i$, K | 366.3 | 366.3 | 366.0 | 366.3 | 366.5 | 366.7 |
| $P_i$, bar | 2.15 | 2.16 | 2.13 | 2.10 | 2.09 | 2.10 |
| $\lambda$ | 1.546 | 1.547 | 1.549 | 1.548 | 1.548 | 1.547 |
| Shaft power, kW | 208.1 | 207.9 | 208.2 | 208.2 | 208.1 | 208.0 |
| LHV, MJ/m$^3$ | 32.042 | 31.379 | 30.741 | 29.771 | 28.699 | 27.792 |
| Wobbe, MJ/m$^3$ | 44.286 | 44.021 | 43.771 | 43.414 | 42.998 | 42.646 |
| KLST, °BTDC | 23.0 | 22.0 | 21.0 | 19.5 | 18.0 | 17.0 |
| MN, AVL | 89.8 | 91.7 | 89 | 84 | 79.4 | 75.5 |

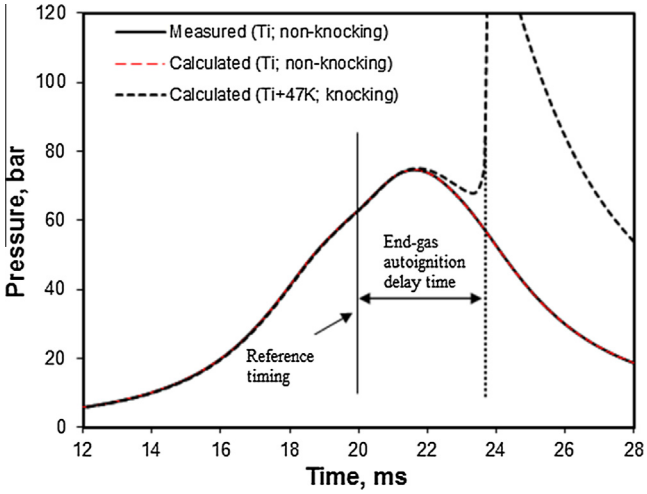


**Fig. 1.** Measured pressure history and calculated autoignition of Gas A using the complete measured pressure and derived temperature history, at both the actual intake manifold temperature $T_i$ and at $T_i + 47$ K.

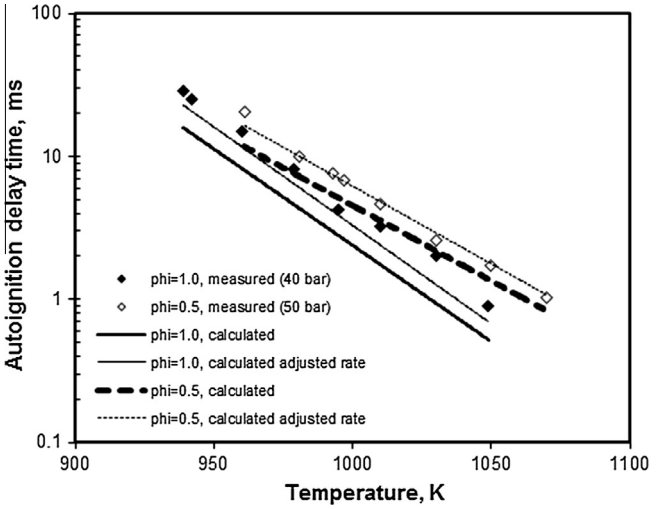


**Fig. 2.** Measured and calculated autoignition delay time as function of temperature for fuel lean ($\varphi = 0.5$) and stoichiometric methane/hydrogen (70:30) mixtures. The points denote the experimental results, while the lines show the best-fit line through the computed delay times. The dashed ($\varphi = 0.5$) and solid ($\varphi = 1.0$) lines denote calculations performed with the original mechanism (bold lines) and those using the reduced rate constant of reaction (thin lines).

resistance than the reference Gas A should, and do, show autoignition earlier in the cycle. For the purposes of analysis, it will be convenient to define an ignition delay time for the end gas, analogous to RCM measurements, taken from some reference point. Figure 1 shows the definition of the end-gas autoignition delay time in this case.

To compute the end-gas autoignition delay times, we used the mechanism developed in Refs. [10–13]. Previous research (e.g., [12–15]) has shown that this mechanism is able to predict measured autoignition delay times well for methane blends with ethane, propane, butane and pentane under conditions relevant to engines. However, in [14] we observed that the autoignition delay times of methane/hydrogen (70:30) blends measured in a RCM are somewhat underpredicted, as shown in Fig. 2. As also suggested in [16], sensitivity analyses show that reaction

$$H_2 + CH_3O_2 \Longleftrightarrow H + CH_3O_2H, \tag{3}$$

could be responsible for the discrepancy between calculations and measurements shown in Fig. 2. Since reaction (1) demonstrably does not affect the ignition behavior of pure hydrogen or pure hydrocarbon, we altered the expression of the rate coefficient of reaction (1) suggested in [29], $1.5 \times 10^{14}$ exp $(2.603 \times 10^4$ cal/RT) cm$^3$ mol$^{-1}$ s$^{-1}$ by reducing the pre-exponential factor within the reported uncertainty [29], based on a least square fit to the measured autoignition delay times, to $5 \times 10^{13}$ cm$^3$ mol$^{-1}$ s$^{-1}$. The calculated ignition delay times using the new pre-exponential factor are also shown in Fig. 2 and show substantially improved agreement over the measured regime.

## 4. Results and discussion

As will be seen below, variations in gas composition cause a number of significant changes in the in-cylinder conditions affecting autoignition in the end gas. The three main effects discussed here are; the manifestation of the autoignition properties of the chemical composition of the fuel itself [5–18], the changes in thermophysical properties of the fuel–air mixture [20] and the changes in combustion duration, also referred to as combustion "phasing" [21]. After discussing the contributions of these effects to engine knock, we shall proceed to rank the different fuels in terms of knock propensity.

### 4.1. Analysis of the changes in end-gas autoignition with varying gas composition

#### 4.1.1. Autoignition properties of the fuel

We first briefly consider the autoignition delay of different fuel compositions studied here under otherwise identical circumstances. Towards this end, autoignition delay times for the mixtures A, E, F, and G (Table 2) and K and M (Table 3) at a fixed pressure of 75 bar as a function of temperature are presented in Fig. 3. With an eye towards practical lean-burn machines, such as that used in this study, we performed the simulations for fuel-lean conditions ($\varphi = 0.67$).

The fuel mixtures presented in Fig. 3 show the characteristically strong influence of temperature on the ignition delay time; a modest increase in temperature, for example from 900 K to 1000 K, results in a reduction by a factor of roughly five in autoignition delay time. The addition of propane (Mixture F) to reference Gas A (Dutch natural gas, DNG) results in a consistent and substantial decrease in the autoignition delay time over the range of temperature shown in the figure. Interestingly, the addition of ethane (Mixture E) or hydrogen (Mixtures K and M) appears to *increase* the autoignition delay times at temperatures below ~900 K, while at temperatures above ~900 K their addition reduces the autoignition delay time, as expected [5,8,9,15,16,31]. The variation in combined effect of composition with temperature implies that different temperature regimes in different engines can yield quantitatively, and even qualitatively, different knocking behavior in the end gas.

#### 4.1.2. Changes in conditions affecting the state of the end gas

Given the substantial variation in temperature and pressure experienced by the end gas during the cycle, the entire pressure/temperature ($P/T$) history must be included in a detailed analysis of the effects of fuel composition [27,28]. In addition, we must consider the fact that the pressure/temperature history itself can also vary due to varying gas composition. To examine these effects, we measured the pressure profiles of the mixtures presented in Tables 2 and 3 under normal, non-knocking, operating conditions (constant power output, constant spark timing, air ratio controls, etc.). The (averaged) measured pressure traces of the DNG/$H_2$

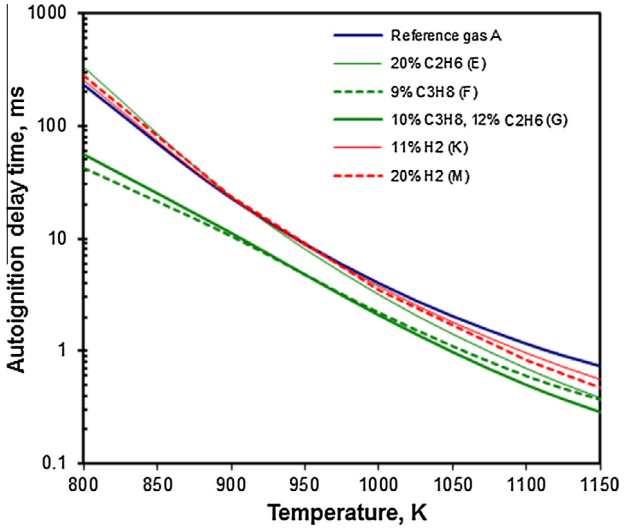


**Fig. 3.** Calculated autoignition delay time as function of temperature for Mixtures A, E, F, G (Table 2), K and M (Table 3), $P = 75$ bar and $\varphi = 0.67$.

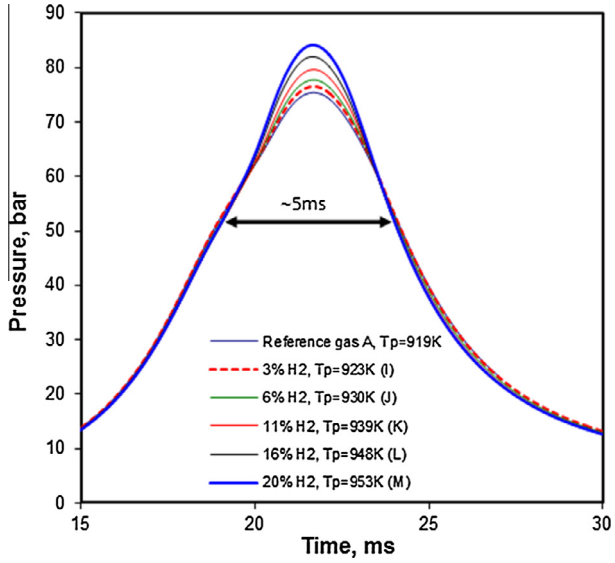


**Fig. 4.** Measured pressure profiles as function of time for DNG/$H_2$ gases (Table 3). In the legend the derived peak temperatures ($T_p$) are presented.

mixtures (Table 3) are presented in Fig. 4. The assumption that the end gas can be treated as adiabatic during combustion, as described in Section 3 [27,28], allows us to calculate the peak temperatures occurring in the unburned mixture by solving Eq. (1) numerically; the resulting temperatures are shown in the legend in Fig. 4.

We note that the peak pressure increases substantially with hydrogen addition, up to 7 bar for 20% $H_2$ in the mixture. This change in peak pressure results in an increase of ~35 K in the peak temperature of the end gas. The origins of this increase in peak pressure and temperature will be discussed below. Before doing so, we first comment on the time scale for autoignition and the combustion duration. Comparing the peak-pressure and -temperature conditions typical for our engine shown in Fig. 4, with the curves shown in Fig. 3, we see that autoignition delay times of greater than ten milliseconds are expected. Since the total combustion duration in this (high-speed) engine is only ~5 ms the engine should be relatively far from its knock point, which it is. To facilitate the discussion regarding knock, below, it will be convenient to

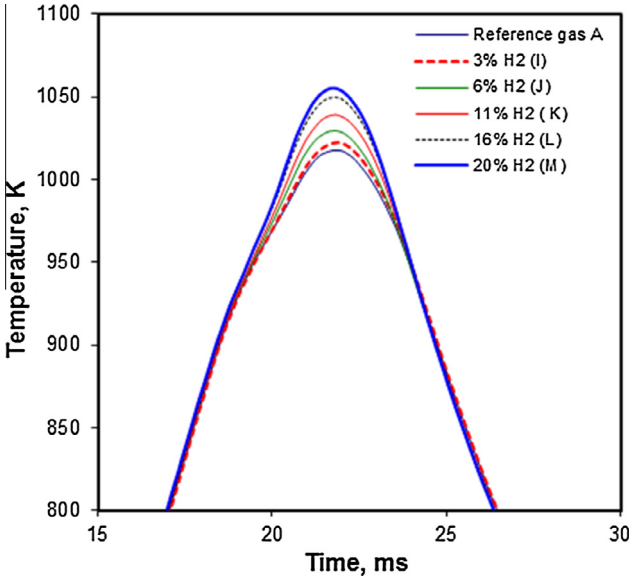


**Fig. 5.** Temperature derived from measured pressure profiles as function of time for DNG/$H_2$ gases (Table 3) by using $T_i + 47$ K in the calculations.

first bring the conditions closer to the knock limit by increasing the initial temperature in the calculations ($T_i$) by 47 K, as done for the knock simulation in Fig. 1. The corresponding temperature histories for the DNG/$H_2$ mixtures are shown in Fig. 5. Here we observe that the pressure increase arising from progressive hydrogen addition results in a similar increase in temperature (to roughly 37 K) than under nominal conditions, but now within the timescale of the combustion duration. With an autoignition delay time for Gas A under the peak conditions of temperature and pressure of roughly 5 ms, we estimate from Fig. 3 that the autoignition delay time for Gas M will then be a factor of two shorter than for Gas A, and bring autoignition of the end gas well into the burn period, which would result in strong knock. Referring to Fig. 3, we see that in this example the effect of hydrogen addition on autoignition of the end gas is twofold: in addition to the (modest) ignition-enhancing effect of 20% hydrogen around 1050 K, the dominant effect is the increase in temperature, by roughly 40 K, exponentially reducing the ignition delay time.

The observed differences in the $P/T$ history upon changes in fuel composition in a modern stationary gas engine are caused by a number of factors. The "trivial" effects are caused by the control system: the fuel–air ratio and the power output are held constant. To maintain constant output, differences in heating value of the fuel (and possibly efficiency) are compensated by changes in the intake pressure. However, the observed differences are mainly caused by in-cylinder conditions, predominantly by changes in burning rate and thermophysical properties (particularly the heat capacity) of the fuel–air mixture.

Clearly, an increase in the burn rate will increase the maximum pressure in the cylinder [1], which in turn increases the temperature of the end gas, enhancing autoignition and knock. However if no change in the burning rate occurs and the compression ratio remains constant (same volume history) it follows from Eqs. (1) and (2) that variation in the composition still affects the $P/T$ history, since $\gamma(T)$, the ratio of temperature-dependent specific heat capacities of the unburned mixture ($C_p/C_v$) changes [20]. Moreover, changes in end-gas pressure and temperature caused by the differences in $\gamma(T)$ will also affect the instantaneous burning velocity during combustion. Thus, we expect the addition of hydrogen to increase the peak pressure/temperature by both the effective reduction in the heat capacity of the end gas and by the increase in the burning velocity itself.

To assess the impact of changes in thermophysical properties and burning rate on the $P/T$ history of the end gas separately, we perform the following exercise, in which we focus on the dominant effect of changes in temperature on the autoignition delay time. To determine the effects of heat capacities on the temperature histories, we must consider the volume history, $V(t)$. Since the initial volume, $V_i$, in Eq. (2) is geometrically defined, this is equivalent to considering CR($t$), the history of the effective compression ratio in Eq. (2). If we assume that the burning velocity of the advancing flame front is independent of composition, then the end gas of all mixtures will be compressed to the same extent during the combustion period. As a result, $V(t)$, and thus CR($t$), of the unburned end gas is assumed identical for all mixtures. Since we use Gas A as a reference, we use the volume history derived from the (non-knocking) pressure history given in Fig. 1, as described in Section 3. Together with the initial temperatures measured for the different gases, increased by 47 K as discussed in relation to Fig. 1, we can use Eq. (2) to calculate the extent to which changes in heat capacity (through the factor $\gamma(T)$) affect the temperature of the end gas as compared to Gas A.[1] This exercise has been performed for Gases G (10% ethane/12% propane) and M (20% hydrogen). The resulting temperature histories are presented in Fig. 6. They show that, although the initial temperature changes only marginally, the peak temperature of the natural gas mixture G, having 10% ethane and 12% decreases substantially, by ~14 K relative to Gas A. The changes in temperature arise from the increase in heat capacity of the mixture caused by the addition of ethane and propane to the fuel, which is predominantly methane. The addition of hydrogen to Dutch natural gas has an opposite effect; addition of 20% hydrogen to Gas A (Gas M) results in an increase in the peak temperature of ~7 K (Fig. 6) at constant compression ratio, caused by the decrease in heat capacity of the mixture upon hydrogen addition. Given the strong sensitivity of spontaneous ignition to temperature, this "thermophysical" effect of the alkanes will be to reduce their effect on autoignition, while the effect of hydrogen will enhance autoignition. This observation is one of the criticisms of using hydrogen/methane mixtures as a measure of knock propensity for alkanes [20]. We note that similar estimates for the pressure history can be made.

In contrast, the temperature profiles derived from the *measured* pressure traces for mixtures G and M, together with Eqs. (1) and (2), are also shown in Fig. 6. Here we see that the peak temperature for Gas G actually *increases* by 7 K with increasing fraction of higher hydrocarbons in the mixture, rather than decreasing by 14 K as described above. The increase in temperature is a result of the increase in burning rate, revealed by the in-cylinder analysis, which causes an increase in the thermal compression (and thus in CR($t$) in Eq. (2)) by the advancing flame front, with larger fractions of higher hydrocarbons in the fuel. From this we conclude that the changes in the combustion "phasing" completely overcome the "thermophysical" effect for these mixtures. Moreover, as can be seen in Fig. 6, the peak temperature for Gas M based on the measurements increases by 37 K, compared to the 7 K increase caused by the purely thermophysical effects upon hydrogen addition. For hydrogen-containing mixtures, we conclude that the changes in CR($t$) caused by changes in combustion phasing have substantially more impact than the changes in the thermophysical properties alone. The in-cylinder analysis shows that 20% hydrogen in DNG reduces the combustion duration by roughly 15%. Measurements reported by others on a cooperative fuel research engine [21,30] also observed a reduction in combustion duration upon hydrogen, ethane and propane addition at constant spark timing. These changes in combustion phasing are also strongly manifested in the pressure histories, as illustrated for example in Fig. 4. Here we remark that the net effect of the addition of ethane and propane to Gas A on the changes in the actual temperature (and pressure) history of the end gas is substantially smaller than the effect of hydrogen addition, as clearly shown in Fig. 6.

#### 4.1.3. Impact of changes on autoignition of the end gas

Having discussed the origins of the differences in the $P/T$ history of the end gas caused by variations in fuel composition, the question arises as to the effects of these changes on the autoignition of the end gas. To quantify these effects, we define the following three cases, shown in Fig. 7. In Case 1 we illustrate solely the effects of the autoignition behavior of the fuels under the same conditions of pressure and temperature. To do so, the autoignition delay times of Gases A, E, F, G, M and K (Tables 2 and 3) are calculated at a constant temperature and pressure corresponding to the peak temperature (1019 K) and peak pressure (75 bar) causing simulated knock at 90% heat release for reference Gas A in Fig. 1. These data are essentially the autoignition delay times for the different mixtures in Fig. 3, taken at 1019 K. In Case 2 we simulate the autoignition delay times based on the peak temperatures and pressures calculated with the maximum effective compression ratio derived for Gas A (as done to obtain the computed curves in Fig. 6). This comparison also includes the (modest) effects of the changes in initial pressure caused by the control system to maintain constant power output. In this way the impact of the changes in thermophysical properties (e.g., $C_p/C_v$) relative to Gas A, which affect the peak-pressure and temperature, on the autoignition behavior is illustrated. Finally, to include the effects of combustion phasing, in Case 3 the autoignition delay times are calculated based on the measured peak pressures and corresponding peak temperatures of the individual gases.

Figure 7 shows that in Case 1 the impact of hydrogen addition (Gases K and M) on the autoignition delay times is modest, as observed in the discussion of Fig. 3, above. However, the ignition promoting effect of hydrogen becomes more pronounced in Case 2, because of the increase in temperature due to the lower heat capacity of the fuel. The effect of hydrogen is even larger in Case 3; the change observed in Case 3 is not only the result of the increase

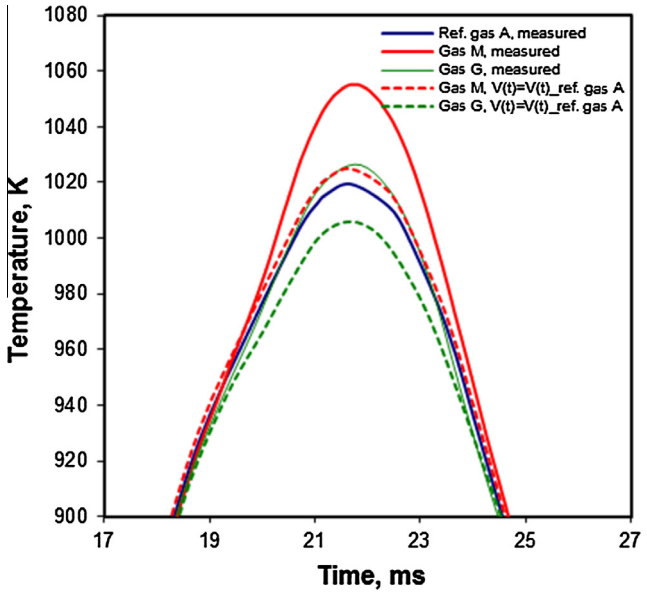


**Fig. 6.** Temperature histories for Gases A, G and M derived from the compression history of reference gas A (dashed lines) and from the measured pressure history (solid lines), using the measured $T_i$ + 47 K and $P_i$ in the calculations (see text).

[1] We recall that, at constant compression ratio, changes in initial pressure result in a different final pressure, but as can be seen in Eqs. (1) and (2) without a change in heat capacity this will have no effect on the gas temperatures.

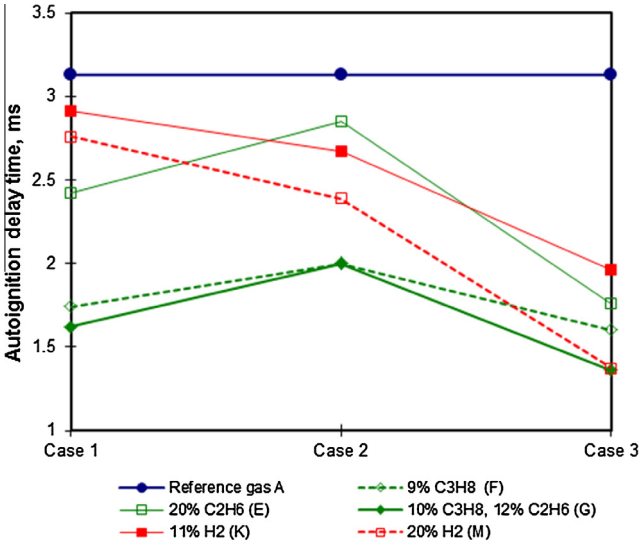


**Fig. 7.** Calculated autoignition delay times for the mixtures A, E, F, G, K and M Tables 2 and 3) for three Cases: Case 1, calculated using the measured peak temperature and pressure from gas A. Case 2, using the peak temperature and pressure derived from the maximum compression ratio of gas A. Case 3, using the measured peak pressure and associated temperature of the mixtures.

in temperature and pressure of the end gas (Figs. 4 and 5) caused by the change in combustion phasing and the heat capacity of the fuel, but also from the fact that the ignition promoting effect of hydrogen becomes larger at higher temperatures, as also shown in Fig. 3. Figure 7 shows that the addition of ethane (Gases E and G) and propane (Gases F and G) to Gas A results in a substantial reduction in the autoignition delay at constant peak pressure and temperature of the end gas (Case 1) as a result of the enhanced chemical reactivity seen in Fig. 3. In Case 2, the autoignition delay time for gases E, F and G are longer than those of Case 1, arising from the decrease in temperature (and pressure) of the end gas with increasing fractions of higher hydrocarbons, caused by the increased heat capacity, as seen in Fig. 6. However, calculations based on the measured peak pressure and corresponding temperature (Case 3) show that in reality the effects of ethane and propane on the combustion phasing, increasing the actual pressure and temperature, shortens the autoignition delay times compared to those in Case 1.

Based on the analyses above, we conclude that the ignition promoting effect of hydrogen is mainly the result of the changes in in-cylinder conditions ($P$, $T$), while the ignition promoting effect of propane and ethane addition to Gas A is predominantly the result of the autoignition kinetics behavior of the fuel itself.

### 4.2. Ranking gases for knock resistance

Given the sensitivity of the autoignition behavior to temperature and pressure illustrated above, to assess the net effects of fuel composition on knock resistance the changes in in-cylinder conditions ($P$, $T$) experienced by the end gas during the combustion cycle must be incorporated in simulations. Towards this end, we rank the gases studied (Tables 2 and 3) for knock resistance based on the autoignition delay times calculated using the complete specific volume history derived from the measured pressure history during the cycle as input in the simulations. The results are plotted in Figs. 8 and 9 as pressure histories. As done in Fig. 1, we raise the temperature of the fuel before compression by 47 K, such that Gas A autoignites ("knocks") at the point in the combustion cycle where 90% of the heat has been released. Autoignition of the end gas at an earlier time indicates that a given fuel has a lower knock

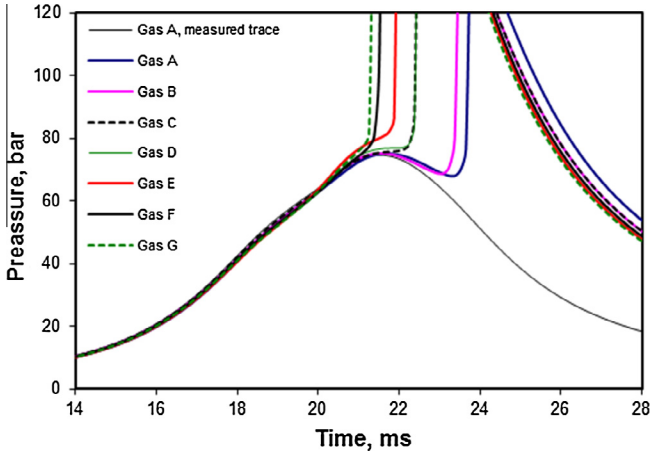


**Fig. 8.** Ignition of the natural gas/ethane/propane mixtures (Table 2) computed using the complete measured pressure and derived temperature history, at initial temperature $T_i$ + 47 K. The non-knocking pressure history for Gas A is also shown.

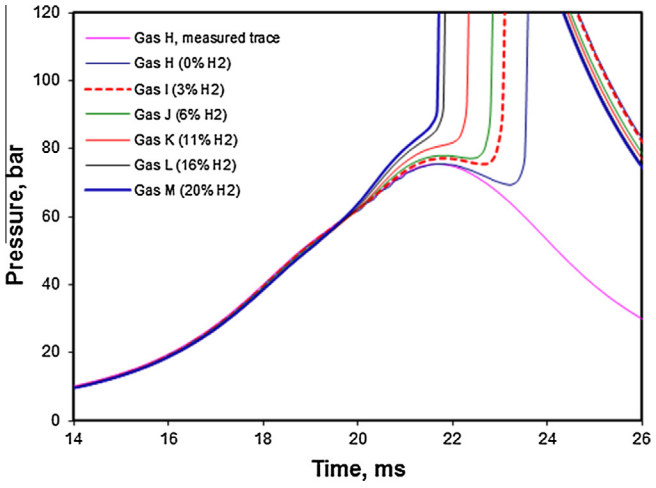


**Fig. 9.** Ignition of $H_2$/natural gas mixtures computed using the complete measured pressure and derived temperature history, at initial temperature $T_0$ + 47 K. The non-knocking pressure history for Gas H is also shown.

"resistance". From these figures, it is clear that the end gas autoignites progressively earlier in the combustion cycle, showing the reduction in knock resistance with increasing fractions higher hydrocarbons (Fig. 8) and hydrogen (Fig. 9) in the fuel.

To explore the relation between the predicted end-gas autoignition as indicator of knock resistance and the measured Knock-Limited Spark Timing (KLST), end-gas autoignition delay times are derived from Figs. 8 and 9 by taking 20 ms as an arbitrary zero, as shown in Fig. 1, and are plotted versus the measured KLST in Fig. 10. When considering the day-to-day variations in the determination of KLST of ±0.75 °CA, we observe an excellent monotonic relationship between the KLST and the calculated end-gas autoignition delay time. From this result we conclude that the simulated end-gas autoignition delay time accurately reflects the measured knock propensity in the high-speed gas engine for the fuel mixtures studied here. Previous work using a similar approach [28] also obtained good predictions of the knock limits when comparing a wide variety of fuels, both liquid and gaseous. We suggest that the ability to discern the knock resistance of gaseous fuels having only "modest" differences in hydrocarbon composition, quantitatively, is a result of the significant advances in the development of accurate chemical mechanisms for autoignition processes for the smaller alkanes (e.g., [9–13]).

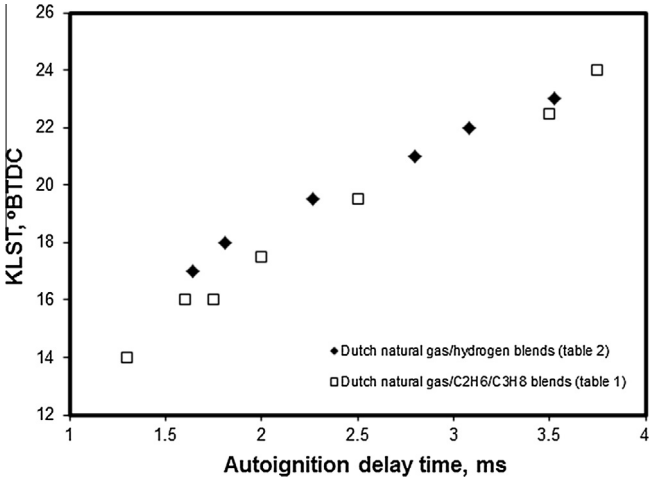


**Fig. 10.** Calculated end-gas autoignition delay time taken from Figs. 8 and 9 versus measured KLST for these mixtures.

We note in passing that comparison of the predictions of knock resistance for the fuels discussed above with those derived from the AVL method for methane number [4], which is widely used in industry, show interesting discrepancies. While for the alkane mixtures (A–G), the AVL method predicts a similar knock resistance to that shown in Fig. 10, the computed methane numbers for Gases H–M severely underestimate the effects of hydrogen on knock seen in our engine, as seen in Table 3 and observed by others [20]. While the origin of this discrepancy may lie in the differences in combustion regime (lean burn in this paper versus stoichiometric in Ref. [4]), in any event it will be clear that circumspection is warranted by the general application of such methods.

## 5. Conclusions

The knock characteristics of natural gas blended with significant fractions of ethane, propane and hydrogen have been studied experimentally and numerically. SENKIN computations of autoignition delay times at 75 bar, typical for the engine studied, as a function of temperature show that the effects of the admixture of different fuel components to a reference natural gas can strongly depend on the temperature. This implies that different temperature regimes in different engines can yield quantitatively, and even qualitatively, different knocking behavior in the end gas.

Experiments in a lean-burn, high-speed medium-BMEP gas engine for CHP have been performed to study the knock behavior of different fuels by keeping following the engine parameters constant, power output, equivalence ratio and engine speed. Analysis of measured non-knocking pressure histories revealed the origins of the variations in temperature and pressure of the end gas upon varying the fuel composition. It was found that changes in the heat capacity and combustion phasing of the fuels significantly changes the pressure and temperature history of the end gas. The effects of these variations on the knocking tendency of the fuel have been assessed using autoignition delay times computed for the end gas under the conditions extant in the engine.

Hydrogen is seen to have a strong impact on the conditions of end gas: the increase in burning velocity (combustion phasing) and the reduced heat capacity of the mixture combine to increase the end-gas temperature and pressure significantly with increasing hydrogen content. Given the progressive increase in the effect of hydrogen fraction on autoignition with temperature, the increase in end-gas temperature amplifies the ignition-enhancing effect of hydrogen itself.

Analysis of the engine measurements shows that the end-gas temperature (and pressure) increases slightly with increasing fractions of ethane and to a lesser extent with propane. Given the increase in the heat capacity with increasing fraction ethane and propane one would naïvely expect a reduction in peak pressure (and temperature) with increasing higher hydrocarbon content. However, analysis of the measured pressure profiles shows that an increase in combustion rate with increasing fraction of higher hydrocarbons caused the observed pressure increase. It should be noted that the effect is more pronounced for ethane than for propane. The strong changes in the autoignition behavior upon admixture of propane, and to a lesser degree ethane, dominate the simulated knock behavior, progressively shortening the end-gas autoignition delay time with increasing admixed fraction.

The effects of the fuel composition can be summarized as follows: the ignition promoting effect of hydrogen is mainly the result of the changes in in-cylinder conditions ($P$, $T$), while the ignition promoting effect of propane and ethane addition is predominantly the result of the enhanced autoignition kinetics of the fuel itself.

Comparison of the computed end-gas autoignition delay time with the measured KLST shows that the computed delay time accurately reflects the measured knock tendency of the fuels. We attribute the ability of the simulations to capture the autoignition effects faithfully for the relatively modest variations in fuel composition discussed here to the major advances in the development of accurate chemical mechanisms for autoignition processes for hydrogen and the smaller alkanes.

## Acknowledgments

This research has been financed by a grant from the Energy Delta Gas Research (EDGaR) program. EDGaR is co-financed by the Northern Netherlands Provinces, the European Fund for Regional Development, the Ministry of Economic Affairs, Agriculture and Innovation and the Province of Groningen. We also gratefully acknowledge the financial support from the N.V. Nederlandse Gasunie.

## References

[1] J.B. Heywood, International Combustion Engine Fundamentals, McGraw-Hill, 1989.
[2] American Society for Testing Materials: Designation D 2699-01a, Standard Test Method for Research Octane Number for spark-Ignition Engine Fuel, 2001.
[3] American Society for Testing Materials: Designation D 2700-01a, Standard Test Method for Motored Octane Number for spark-Ignition Engine Fuel, 2001.
[4] M. Leiker, W. Cartelliere, H. Christoph, U. Pfeifer, M. Rankl, Evaluation of Anti-Knock Property of Gaseous Fuels by Means of the Methane Number and Its Practical Application, ASME paper 72-DGP-4, April 1972.
[5] J. Huang, W.K. Bushe, Combust. Flame 144 (2006) 74–88.
[6] E.L. Petersen, D.M. Kalitan, S. Simmons, G. Bourque, H.J. Curran, J.M. Simmie, Proc. Combust. Inst. 31 (2007) 447–454.
[7] N. Lamoureux, C.E. Paillard, V. Vaslier, Shock Waves 11 (2002) 309–322.
[8] S. Gersen, N.B. Anikin, A.V. Mokhov, H.B. Levinsky, Int. J. Hydrogen Energy 33 (2008).
[9] S. Gersen, A.V. Mokhov, J.H. Darmeveil, H.B. Levinsky, P. Glarborg, Proc. Combust. Inst. 33 (2011) 433–440.
[10] D. Healy, N.S. Donato, C.J. Aul, E.L. Petersen, C.M. Zinner, G. Bourque, H.J. Curran, Combust. Flame 157 (2010) 1526–1539.
[11] D. Healy, N.S. Donato, C.J. Aul, E.L. Petersen, C.M. Zinner, G. Bourque, H.J. Curran, Combust. Flame 157 (2010) 1540–1551.
[12] D. Healy, M.M. Kopp, N.L. Polley, E.L. Petersen, G. Bourque, H.J. Curran, Energy Fuels 24 (2010) 1617–1627.
[13] D. Healy, D.M. Kalitan, C.J. Aul, E.L. Petersen, G. Bourque, H.J. Curran, Energy Fuels 24 (2010) 1521–1528.
[14] S. Gersen, J.M. Darmeveil, H.B. Levinsky, Combust. Flame 159 (2012) 3472–3475.
[15] Y. Yu, G. Vanhove, J.F. Griffiths, S. De Ferrières, J.F. Pauwels, Energy Fuels 27 (2013) 3988–3996.
[16] J. Huang, W.K. Bushe, P.G. Hill, S.R. Munshi, Int. J. Chem. Kinet. 38 (2006) 221–233.
[17] Y. Zhang, Z. Huang, L. Wie, J. Zhang, C.K. Law, Combust. Flame 159 (2012) 918–931.
[18] L.J. Spadaccini, M.B. Colket III, Prog. Energy Combust. Sci. 20 (1994) 431–460.

[19] G.A. Karim, S.R. Klat, J. Inst. Fuel 39 (1966) 109–119.
[20] A.A. Attar, G.A. Karim, Trans. ASME 125 (2003) 500–504.
[21] S.O. Bade Shrestha, G.A. Karim, Proc. Inst. Mech. Eng. 215 (2001) 63–73.
[22] Z. Huang, B. Liu, K. Zeng, Y. Huang, D. Jiang, X. Wang, H. Miao, Energy Fuels 21 (2007) 2594–2599.
[23] M. Baretta, A.E. Catania, E. Spessa, A. Vassallo, ASME paper ICEF: 2005-1216, 2005.
[24] J. Tagalian, B. Heywood, Combust. Flame 64 (1986) 243–246.
[25] E. Lutz, R.J. Kee, J.A. Miller, SENKIN: A FORTRAN Program for Predicting Homogeneous Gas Phase Chemical Kinetics with Sensitivity Analysis. Sandia National Laboratories, Report No. SAND 87-8248, 1988.
[26] R.J. Kee, F.M. Rupley, J.A. Miller, CHEMKIN II: A Fortran Chemical Kinetics Package for the Analysis of Gas-Phase Chemical Kinetics, Sandia National Laboratories, 1989.
[27] K.M. Chung, J.B. Heywood, J.C. Keck, Proc. Combust. Inst. 22 (1988) 455–463.
[28] P.D. Ronney, M. Shoda. S.T. Waida, C.K. Westbrook, W.J. Pitz. International Fuels and Lubricants Meeting and Exposition, SAE Paper 912311, 1991.
[29] W. Tsang, R.F. Hampson, J. Phys. Chem. Ref. Data 15 (1986) 1087–1279.
[30] G.A. Karim, I. Wierzba, Y. Al-Alousi, Int. J. Hydrogen Energy 21 (1996) 625–631.
[31] N. Donohoe, A. Heufer, W.K. Metcalfe, H.J. Curran, M.L. Davis, O. Mathieu, D. Plichta, A. Morones, E.L. Petersen, F. Güthe, Combust. Flame 161 (2014) 1432–1443.